EAGE

NFR07

A Geologically Consistent Permeability Model of Fractured Folded Carbonate Reservoirs: Lessons from Outcropping Analogue

K. Bisdom* (Delft University of Technology), G. Bertotti (Delft University of Technology), B.D.M. Gauthier (TOTAL S.A.) & N.J. Hardebol (Delft University of Technology)

SUMMARY

Presently adopted fracture-related permeability models of large folded reservoirs are simplistic and often unrelated to the geological setting and evolution of the considered structure. In order to improve predictions of fluid flow in more complex subsurface fractured reservoirs, we build a 3D fracture network model of an outcropping fold in Tunisia, and populate different structural domains with fracture data, collected from outcrops.
Within the studied fold, we find large variations in deformation mechanisms between different formations, with the main mechanisms being Layer Parallel Shortening (LPS), resulting in regional deformation, and the more localized impact of fiber stresses and flexural slip. Within the steep flank of the anticline, we find that in one formation fracturing is mostly controlled by fiber stresses, whereas in the underlying formation flexural slip is the main deformation mechanism. These two formations are separated by a detachment surface.
Using stress and strain fields, we aim at reconstructing the conditions at which these fractures have been formed. This can provide a better understanding of the relation between fracture patterns in different structural domains of a fold and the stress evolution that formed these fractures, and the subsequent impact of different fracture patterns on fluid flow in fractured folds.

Introduction

Presently adopted fracture-related permeability models of large folded reservoirs are simplistic and often unrelated to the geological setting and evolution of the considered structure. Fractures are modelled in simplistic undeformed reservoirs where their intensity and orientation is sometimes related to nearby large-scale faults, but the relation with folding and the resulting development of fractures is only indirectly quantified by for example using curvature as a driver for fracture intensity (e.g. (Hillis, 1998)). This method is effective in predicting fracture patterns in relatively simple structures (e.g. (Ericsson et al., 1998)), but in more complex structures, such as fault-propagation folds, curvature alone is not a representative proxy of fracturing (e.g. (Cooke et al., 1999)). As a result, fracture heterogeneity is often simplified or overlooked, especially when only limited subsurface fracture data is available.

Our goal is to build a detailed geological and reservoir model of a surface fractured anticline in order to better understand the impact of a geologically more complex structure on the 3D anisotropy of a fracture network and the subsequent impact on effective fracture network permeability. Eventually we want to perform fluid flow simulations on the constructed geological fracture models in order to assess the sensitivity of fracture geometric (e.g. size, spacing, orientation) and diagenetic (aperture, burial depth) attributes with respect to fluid flow.

We build models of outcropping analogue fractured carbonates, opposed to subsurface models using subsurface well data, as well data is often sparse an not able to fully capture the fracture network heterogeneity (Gauthier, 2003). Outcrops on the other hand provide the 2.5D (i.e. including fracture orientation) characteristics of fractures and are ideal for studying fracture patterns in complex structures such as fault-propagation folds, and their impact on permeability models of fractured reservoirs.

The fault-propagation fold model is built using large-scale 3D modelling and then populated with fracture data collected from different structural domains. We interpret the fractures with relation to the large-scale fold development, and use the resulting stress fields from the reconstruction to extrapolate fracture characteristics from the outcrops to a complete 3D fracture network suitable for use in fluid flow simulations.

Data acquisition and interpretation

The outcropping analogue

We acquire fracture outcrop data from four anticlines in the Southern Atlas in central Tunisia, in the foothills of the Tunisian Tell Mountains, an extension of the North African Atlas domain (Figure 1). The outcropping structures in this region are suitable analogues to subsurface reservoirs in Libya and southern Tunisia. The fieldwork region is confined by two major strike-slip faults. This region is under NNW-SSE to N-S compression since the Aptian age (Bouaziz et al., 2002). Development of the Chotts range started in the Late Cretaceous, while folding of the other structures started in the Miocene (Saïd et al., 2011). Folding is still active today under a similar tectonic N-S regime (Gharbi et al., 2013).

The anticlines provide excellent exposures of Eocene and Upper-Cretaceous fractured carbonates and their geometries are clearly defined in 3D, enabling us to quantify the multi-scale relations between large-scale fold geometry, seismic-scale faults and small-scale deformation features such as fractures and stylolites. We focus initially on the Alima anticline, which is an E-W trending anticline with a fold axis length of 20 km. The anticline has a gently dipping northern flank (10-20°) while the southern flank is faulted and folded, creating a steep nearly overturned limb, providing both sub-horizontal layers and sub-vertical tilted layers.

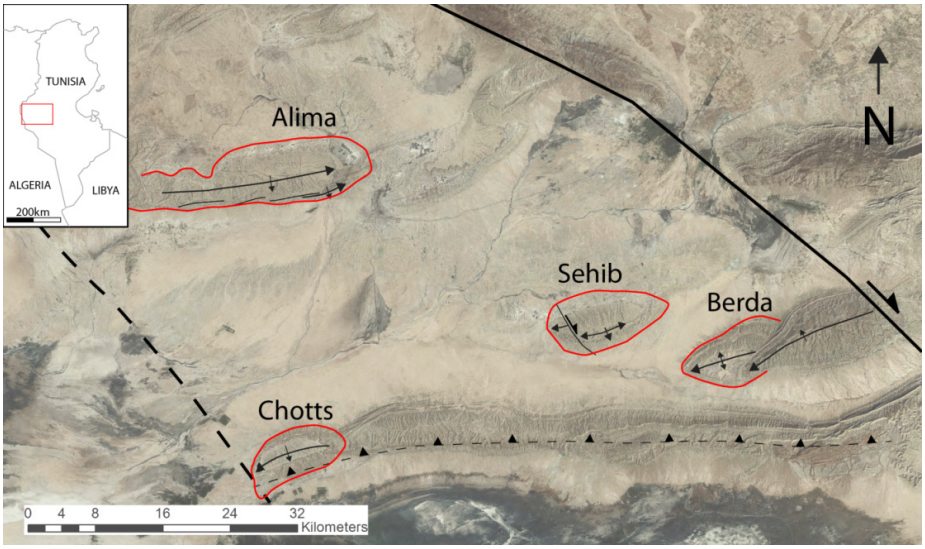

Figure 1 *Location map showing the four anticlines of interest, confined in the west and east by two major strike-slip faults.*

The geometric model

Large-scale geometrical modelling is done using 2D seismic sections, satellite imagery, Digital Elevation Maps and geological maps, which are all data sources that have a similar resolution compared with subsurface methods (e.g. seismic). All data is combined and extrapolated to a 3D model using Gocad geo-modelling software.

Fracture data collection

We collect small-scale deformation data in the field by georeferencing outcrop images in a GIS-based software tool Digifract, on which we digitize all visible fractures. Fracture attributes (e.g. orientation, movement, infill) are also measured directly in the field, resulting in a 2.5D database of oriented fracture traces from which we can immediately extract fracture statistics such as spacing, size and orientation sets. By digitizing also the bedding features, we quantify the impact of a potential mechanical stratigraphy on the fracture set development. Digifract datasets are also exported to Gocad geo-modelling software to place the outcrop data in the 3D model and extrapolate the fracture traces to 3D surfaces with their corresponding orientation.

During a 2-week field campaign we digitize 2100 fractures, veins and stylolites with their corresponding attributes, in addition to bedding surfaces, in 25 outcrops in different structural domains of all four anticlines. We digitize both fracture heights and lengths by including fractures on sub-vertically dipping outcrops. Outcrop size varies from m-scale to km-scale, resulting in a range of fracture sizes from cm to km. In all outcrops we distinguish multiple sets based on orientation, and calculate for all sets the fracture intensity using the processing tools in our fracture digitizing tool. We correct the spacing distribution for orientation bias using the Terzaghi correction and remove censored fractures from the size distribution.

Results

Fracture characteristics

In the Alima anticline we find that structures develop at three different stages driven by three different mechanisms. Mode I fractures developed during Layer Parallel Shortening (LPS). They are sub-perpendicular to bedding, often organized in two orthogonal sets parallel and perpendicular to the fold axis with a large height or length (up to 150 m), where height is not confined by bedding. Flexural slip along the flanks of the anticline was important and caused the formation of mode I fractures as well as stylolites; both are characteristically oblique to bedding, small, and generally bed-confined. Fracturing related to fibre stresses is subordinate and concentrated in the very localized sharp hinges.

The fracture length and height distributions of both LPS and flexural-slip related features follow negative exponential distributions. Spacing on the other hand follows a normal distribution, indicating that the fracture sets are spatially saturated (Rives et al., 1992). For fibre stress related fractures we require more data to accurately establish the relations. Based on orientations, we divide the LPS and flexural-slip fractures in 5 sub-vertical and 3 oblique-to-bedding sets. Fractures belonging to the sub-vertical sets are larger than those in the oblique-to-bedding sets, but there is not yet sufficient data to calculate the exact fracture size and spacing distributions per set.

Fold-scale stress-strain field

In order to create a fracture network permeability model we need to extrapolate the outcrop data to a fold-scale fracture network. The extrapolation from 2D outcrops to 3D models is done by using a 3D principal stress field as the main driver for fracture orientation and intensity. We derive the 3D stress field through mechanical modelling.

We use palinspastic reconstructions to model the principle stress field in different stages of folding and compaction, conditioned to the different types of fractures found in the Alima anticline and their corresponding intensity and orientation. The reconstructions are done using 3D Move software. The resulting stress fields are the main drivers to extrapolate fracture sets measured in outcrops to full 3D fracture networks covering the entire anticlines (Figure 2). Making use of Abaqus mechanical modelling software we model the stress state in different stages of folding in the 3D anticline, deriving proxies for both fracture intensity and fracture orientation.

The 3D stress maps serve as a drivers to extrapolate 2D outcrop data to a 3D fracture network, similar to the subsurface approach where 1D well data is extrapolated using a range of geological or mechanical drivers. We also include seismic-scale faults as a potential driver, to test the assumption often made in subsurface studies that faults are sufficient drivers for fractures, without incorporating other geological knowledge. We validate our mechanical interpretations with a second fieldwork to collect additional fracture data from new outcrops to test whether the outcrop data matches the mechanical development predicted by our models.

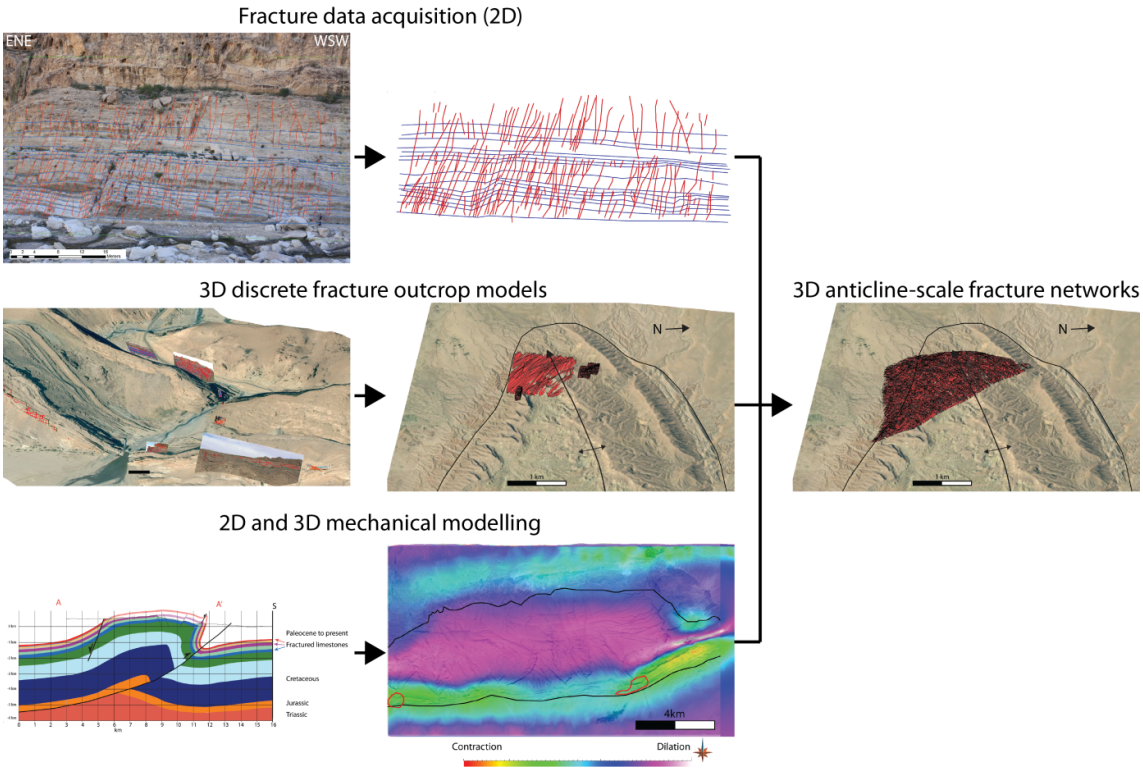

Figure 2 *Outcrop-based workflow to build detailed 3D fracture networks using i) large and statistically complete 2D fracture datasets; ii) extrapolation of 2D fractures in 3D volumes confined to small regions around the outcrops; iii) 2D palinspastic restorations and 3D mechanical modelling provides 3D stress fields serving as drivers for fracture extrapolation.*

From fracture networks to physical properties and fluid flow models

The extrapolation to a 3D fracture network is done through two different methods to test which method has the highest accuracy: i) an explicit method using small DFN models conditioned locally to outcrops and the 3D stress field to build an anticline-scale Discrete Fracture Network and ii) an implicit method using fracture set characteristics and the 3D stress field to populate an anticline-scale grid with effective permeability values. Validation of the methods is done by collecting more data in the field.

The anticline-scale 3D fracture networks serve as the base for both connectivity analysis and more detailed matrix-fracture fluid flow modelling, with the goal of quantifying the accuracy of quick connectivity analysis (e.g. pathway and cluster analysis, streamlines) compared to complex matrix-fracture fluid flow models using highly detailed and geologically accurate (i.e. unstructured or surface-based) grids. Simultaneously, we use these models to quantify the uncertainty in different fracture geometric and diagenetic attributes and their impact on fluid flow.

Acknowledgements

We thank TOTAL S.A. for their funding for this project. We are grateful to the University of Sfax in Tunisia for their support in the field. For the use of their software we are grateful to Paradigm for GOCAD/SKUA and Golder Associates for FracMan, as well as Midland Valley for 3D Move.

References

Bouaziz, S., Barrier, E., Soussi, M., Turki, M.M. and Zouari, H. [2002] Tectonic evolution of the northern African margin in Tunisia from paleostress data and sedimentary record. *Tectonophysics*, **357**, 227-253.

Cooke, M.L., Mollema, P.N., Pollard, D.D. and Aydin, A. [1999] Interlayer slip and joint localization in the East Kaibab Monocline, Utah: field evidence and results from numerical modelling. *Geological Society, London, Special Publications*, **169**, 23-49.

Ericsson, J.B., McKean, H.C. and Hooper, R.J. [1998] Facies and curvature controlled 3D fracture models in a Cretaceous carbonate reservoir, Arabian Gulf. Geological *Society, London, Special Publications*, **147**, 299-312.

Gauthier, B.D.M. [2003] Full Field Fracture Modeling: an Integrated Approach with Application to three Carbonate Fractured Reservoirs: AAPG Hedberg Conference "Paleozoic and Trisassic Petroleum Systems in North Africa".

Gharbi, M., Masrouhi, A., Espurt, N., Bellier, O., Amari, E.A., Ben Youssef, M. and Ghanmi, M. [2013] New tectono-sedimentary evidences for Aptian to Santonian extension of the Cretaceous rifting in the northern Chotts range (southern Tunisia). *Journal of African Earth Sciences*, **79**, 58-73.

Hillis, R.R. [1998] The influence of fracture stiffness and the in situ stress field on the closure of natural fractures. *Petroleum Geoscience*, **4**, 57-65.

Rives, T., Razack, M., Petit, J.P. and Rawnsley, K.D. [1992] Joint spacing: analogue and numerical simulations. *Journal of Structural Geology*, **14**, 925-937.

Saïd, A., Baby, P., Chardon, D. and Ouali, J. [2011] Structure, paleogeographic inheritance, and deformation history of the southern Atlas foreland fold and thrust belt of Tunisia. *Tectonics*, **30**, TC6004.